Pharmaceutical Research, Vol. 25, No. 2, February 2008 (© 2007)
DOI: 10.1007/s11095-007-9466-2

Research Paper

Core–shell Particles for the Dispersion of Small Polar Drugs and Biomolecules in Hydrofluoroalkane Propellants

Libo Wu,[1] Balaji Bharatwaj,[1] Jayanth Panyam,[2] and Sandro R. P. da Rocha[1,3]

Received July 13, 2007; accepted October 1, 2007; published online October 17, 2007

Purpose. Demonstrate the applicability of a novel particle-based technology for the development of suspensions of small polar drugs and biomolecules in hydrofluoroalkane (HFA) propellants for pressurized metered-dose inhalers (pMDIs).
Materials and Methods. Emulsification diffusion was used to prepare core–shell particles. The shell consisted of oligo(lactide) grafts attached onto a short chitosan backbone. The active drug was arrested within the particle core. Colloidal Probe Microscopy (CPM) was used to determine the cohesive forces between particles in a model HFA propellant. The aerosol characteristics of the formulations were determined using an Anderson Cascade Impactor (ACI). Cytotoxicity studies were performed on lung epithelial and alveolar type II cells.
Results. CPM results indicate that particle cohesive forces in liquid HFA are significantly screened in the presence of the polymeric shell and correlate well with the physical stability of suspensions in propellant HFA. The proposed formulation showed little or no cytotoxic effects on both Calu-3 and A549 cells.
Conclusions. Core–shell particles with a shell containing the lactide moiety as the HFA-phile showed excellent dispersion stability and aerosol characteristics in HFA-based pMDIs. This is a general strategy that can be used for developing novel suspension pMDIs of both small polar drugs and large therapeutic molecules.

KEY WORDS: biomolecules; colloidal probe microscopy; pressurized metered-dose inhaler; pulmonary drug delivery; salbutamol sulfate.

INTRODUCTION

In spite of the recognized potential advantages in delivering large therapeutic molecules such as peptides, DNA and proteins through the pulmonary route (1–9), Exubera® is the only inhalation formulation approved by the FDA for the delivery of a systemically acting biomolecule (insulin) (10). Studies have indicated that biomolecules are generally more bioavailable when delivered through the lungs than any other port of entry to the body (1,5,7). This has been attributed to the intrinsic properties of the alveolar region (1). Other major advantages of inhalation therapy include its noninvasive nature and the absence of first pass metabolism (4). The rate of absorption of biomolecules from the lungs into the circulation system is known to vary inversely to their molar mass (7). Small peptides and proteins, such as insulin, reach the circulation system within minutes after inhalation, while larger proteins (>40 kDa) are absorbed relatively slowly (in the order of hours) (11,12). The fact that the lungs still represent a relatively unexploited site for the delivery of large therapeutic molecules can be attributed, to a large extent, to challenges in the development of appropriate inhalation formulations (3,5,10,13–15).

Pressurized metered dose inhalers (pMDIs) are the least expensive and most widely used devices for the delivery of drugs to the lungs (8,14,16–18). pMDIs are, therefore, potential candidate devices for the development of formulations containing large therapeutic molecules. However, both small and large polar solutes, including water and biomolecules, have very limited solubility in the hydrofluoroalkane (HFA) propellants accepted for use in pMDIs (8,19). Therapeutic molecules with low solubility in the propellant HFAs have to be thus generally formulated as suspensions. However, none of the hydrogenated amphiphiles used to stabilize micronized drug particles in the previously marketed CFC-based formulations have appreciable solubility in HFAs (16), compounding the difficulties in preparing dispersion-based pMDIs. HFAs are the non-ozone depleting replacements to CFCs. Co-solvents, usually alcohols, have been instrumental in curtailing surfactant solubility issues (19), and have thus helped in the formulation of small drug molecules in HFA-based pMDIs (8,14). More recent studies have attempted to demonstrate the ability of surface active compounds containing highly HFA-philic groups to stabilize drug suspensions in the low dielectric HFAs without the use of co-solvents (14,20–24). However, it is not clear whether traditional surfactant-stabilized dispersions can be extended to larger therapeutic biomolecules.

[1] Department of Chemical Engineering and Materials Science, Wayne State University, Detroit, Michigan, USA.
[2] Department of Pharmaceutical Sciences, Wayne State University, Detroit, Michigan, USA.
[3] To whom correspondence should be addressed. (e-mail: sdr@eng.wayne.edu)

There have been several publications discussing novel particle formation technologies to systems of relevance to pMDIs (14,20–24). The techniques can be divided in those that attempt to control either the morphology (21,24,25), or chemistry (22,23) of the particles. For example, very good dispersion stability can be achieved with porous drug particles. The propellant molecules can penetrate into the pores of the particles, thus reducing the van der Waals attractive forces (20). However, only 50 wt % or less of the content of the porous particles are active ingredients. Lipid-coated budesonide microcrystals with high degree of surface roughness prepared by spray drying were shown to possess improved suspension stability in HFA134a (24). The physical stability of the particles in that case was not significantly improved compared with traditional micronized formulations. It has been also demonstrated that the addition of poly(vinyl alcohol) (PVA) during spray drying could enhance the colloidal stability of protein particles in HFA134a (22,23). The enhancement in the stability of the suspension was attributed to a change in surface chemistry of the particles (22,23).

One of the main mechanisms for imparting stability to colloidal particles in low dielectric solvents such as HFA propellants is steric stabilization (14). Steric stabilization is dominated by solvation effects (26), and may be achieved by selecting amphiphiles that have an anchor segment that strongly interacts with the dispersed phase, and a well-solvated tail segment that extends into the bulk/dispersing medium. We have used a combined computational and experimental approach to probe the solvation of promising tail moieties in hydrofluoroalkanes at the microscopic level (27,28). *Ab intio* calculations and chemical force microscopy (CFM) were used to determine the enthalpic interactions between HFA and moieties of interest, thus developing a quantitative relationship between chemistry of candidate stabilizing groups and HFA-philicity (27,28). The ability of amphiphiles and surface modification techniques in screening the cohesive forces between drug crystals, thus providing enhanced suspension stability, has been investigated by Colloidal Probe Microscopy (CPM) (29–32).

The goal of this work is to demonstrate the applicability of a novel particle-based technology for the development of stable suspensions of both small polar solutes and large therapeutic molecules in hydrofluoroalkane propellants. We use a single step, low energy input method for preparing core–shell particles where the active drug is located within the particle core, and the shell consists of a copolymer with biodegradable blocks carefully designed to encapsulate the drug and to enhance the stability of the dispersion in HFAs. We tested the effectiveness of the surface modification in screening the cohesive forces between drug particles by directly probing the forces of interaction between particles by CPM. The physical stability and aerosol characteristics of the core–shell particles in HFA propellants were also tested. The cytotoxicity of the formulation was investigated in Calu-3 and A549 lung cell lines.

MATERIALS AND METHODS

Materials. Chitosan (CS, medium molecular weight) was purchased from Aldrich Chemicals Ltd. D,L-lactide was obtained from Frinton Laboratories, Inc., and was recrystallized twice from ethyl acetate. Stannous octoate was purchased from Sigma. 2H, 3H-perfluoropentane (HPFP) was purchased from SynQuest Labs Inc (purity of 98%). The hydrofluoroalkanes 1,1,1,2,3,3,3-heptafluoropropane (HFA227), and 1,1,1,2-tetrafluoroethane (HFA134a) (pharma grade, purity >99.99%) were a gift from Solvay, Inc. Salbutamol Sulfate (SS) was purchased from Spectrum Chemicals. Bovine serum albumin (BSA) was purchased from Sigma. Hydrogen peroxide was from Fisher Chemicals. The Calu-3 cell line was purchased from ATCC (Manassas, VA). Dulbecco's Modified Eagle's Medium (4,500 mg L^{-1} glucose, 110 mg L^{-1} sodium pyruvate) was purchased from Sigma. RPMI 1640 supplemented with L-glutamine was obtained from Invitrogen. The A549 human lung carcinoma cell line was obtained from Prof. Sujatha Kannan's laboratory at Wayne State University. DMEM and RPMI 1640 were supplemented with 10% fetal bovine serum (FBS) and 100 μg ml^{-1} penicillin and streptomycin, both purchased from Sigma. Culture flasks (75 cm^2, BD-falcon) were purchased from VWR. 96-well culture plates were obtained from Corning. MTS [(3-(4, 5-dimethylthiazole-2-yl)-5-(3-carboxymethoxyphenyl)-2-(4-sulfophenyl)-2H-tetrazolium, inner salt] was purchased from Promega. Deionized water (NANOpure® DIamond™ UV ultrapure water system: Barnstead International), with a resistivity of 18.2 MΩ cm and surface tension of 73.8 mN m^{-1} at 296 K, was used in all experiments. Two-component Epoxy (Epotek 377) was from EPO-TEK. All the other organic solvents were supplied by Fisher Chemicals and were of analytical grade. NP-20 Si_3N_4 V-shape contact mode cantilevers with integrated pyramidal tips were purchased from Veeco Instruments.

Degradation of Chitosan. A known amount (8 g) of CS was dissolved in 200 ml DI-water with the aid of hydrochloric acid, and heated to 353 K for 3 h. A 10 ml hydrogen peroxide solution (30%) was subsequently added to the CS aqueous solution. The mixture was kept at 353 K for another 12 h to degrade the long chain CS to smaller (water-soluble) oligomers (33). The pH of the degraded CS solution was then adjusted with NaOH to neutral. CS was precipitated into a large volume of ethanol. The water-soluble CS oligomer was then collected by centrifugation, and dried in air at room temperature. The number average molecular weight (Mn) of the degraded CS powder was determined by size exclusion chromatography (SEC) using a Shimadzu LC-10ADVP liquid chromatograph equipped with a seven-angle static light scattering detector (BIMwA) and differential refractometer (BIDNDC), both from Brookhaven Instruments, Inc.

Synthesis of Oligo(lactide)-grafted-chitosan (LA-g-CS). The synthesis of the LA-*g*-CS copolymer is illustrated in Scheme 1. Briefly, 0.4 g of degraded CS, 4 g D,L-lactide, and an appropriate amount of stannous octoate were added into 40 ml of toluene under magnetic stirring. The reaction was carried out at 373 K under nitrogen atmosphere for 24 h. The resultant products were then centrifuged and the precipitate was collected and washed with acetone repeatedly to give the final product (34). ^{1}H NMR (Varian Mercury 400) and FTIR (Bruker Tensor 27) were conducted to confirm the molecular structure of the LA-*g*-CS copolymer.

Preparation of the Core–shell Particles. Particles were prepared by emulsification–diffusion. Briefly, 25 mg of the molecule of interest was first dissolved in 0.8 ml of water. The

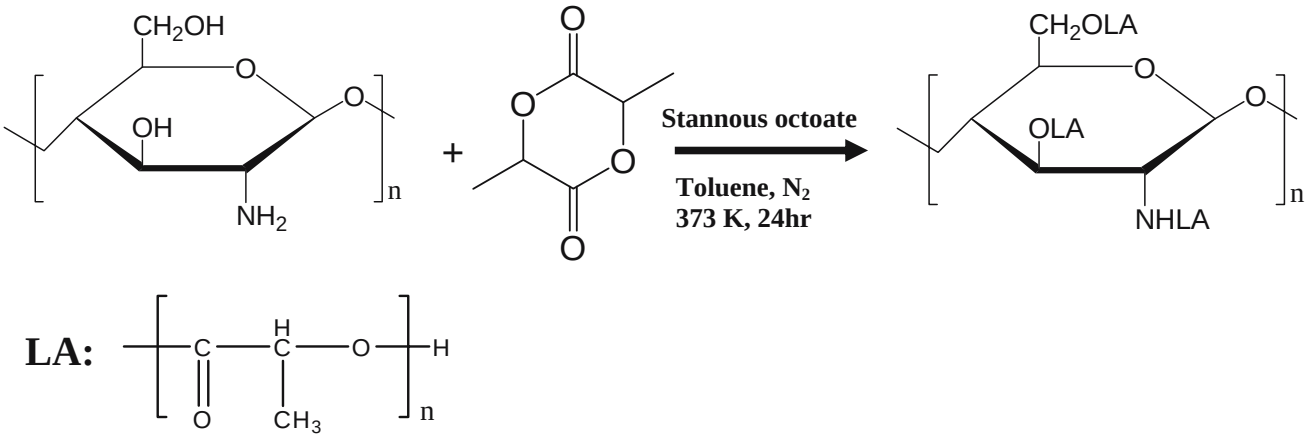

Scheme 1. Scheme for the synthesis of oligo(lactide)-*g*-chitosan copolymer.

aqueous solution was then emulsified in 19 ml of ethyl acetate using a sonication bath (VWR, P250D, set to 180 W). A water-in-oil (W/O) emulsion was thus obtained. The emulsion was subsequently added to a large volume (150 ml) of ethyl acetate. The particles were formed as water that makes the dispersed emulsion phase diffuses out into ethyl acetate, and collected by centrifugation. Core–shell particles, where the shell is made of the LA-*g*-CS copolymer, and the core is the polar compound (in our case either SS or BSA) were also prepared by emulsification–diffusion. Briefly, 25 mg of the compound of interest and 12 mg LA-*g*-CS copolymer were dissolved in 0.8 ml water. The aqueous solution was then emulsified in 19 ml ethyl acetate using a sonication bath (same conditions as before). The obtained W/O emulsion was then transferred into 150 ml ethyl acetate. The LA-*g*-CS core–shell particles were formed by the same mechanism as described above. They were collected by centrifugation, and dried at room temperature.

Characterization of the Size and Morphology of the Core–shell Particles. The particle size and morphology was analyzed by scanning electron microscopy (SEM, Hitachi S-2400). Core–shell particles prepared as discussed above were first dispersed in HPFP by sonication. Several drops of the particle suspension in HPFP were placed on a cover glass slip and allowed to dry. The cover glass substrates were then sputtered for 30 s with gold for SEM analysis. The core–shell morphology of the particles was investigated on a transmission electron microscope (TEM, JEOL JEM-2010). A drop of the core–shell particle dispersion in HPFP was added onto a 200-mesh copper grid and then dried in air for TEM analysis.

Preparation of the Particle-modified AFM Probe. Single particles were glued onto silicon nitride contact-mode cantilevers (NP-20) with the help of an AFM (Pico LE, Molecular Imaging). The two components of the epoxy (Epotek 377) were mixed and heated to 353 K in a water bath for 30 min, until it became highly viscous. A small drop of epoxy was then transferred onto a piece of silicon wafer. The AFM cantilever was first positioned above the drop of epoxy with the help of a CCD camera. The AFM tip was then slowly brought into contact with the substrate until a very small amount of epoxy was transferred. A similar procedure was used to attach a single particle to the tip of the AFM cantilever containing the epoxy. The particle-modified AFM tip was then kept at room temperature inside a desiccator for 24 h to allow complete curing of the epoxy. The spring constant of the particle-modified cantilever was determined using a module attached to the AFM and the MI Thermal K 1.02 software. SEM images of the modified cantilevers were obtained after the cohesion force measurements were performed.

Colloidal Probe Microscopy (CPM). The cohesive force between particles was probed directly by CPM. CPM is an AFM-based technique where the force of interaction between a particle-modified AFM tip and another particle/substrate is measured in air/liquid, with pico newton accuracy (35). The cohesion force (F_{co}) is defined as the product of the spring constant of the particle-modified AFM cantilever and the maximum cantilever deflection during the retraction stage of the force measurement. A fluid cell was used to conduct the CPM experiments in liquid HPFP at 298 K. HPFP has been proposed as a mimicking solvent to propellant HFAs.(29–32,36,37) Drug particles were initially deposited onto a silicon wafer from HPFP. The adhesive force between the particles and the substrate is stronger than that between particles, so that the particles remain bound to the substrate during the measurements. Several randomly distributed particles on the substrate were selected for the F_{co} measurements. For each contact point between the two particles, 25 force–distance curves were recorded in a range of 2,000 nm, and the sweep duration of 2 s. The histogram of the measured F_{co} was fit to a Gaussian distribution, from which an average force and deviation was obtained.

Interfacial Tension. The interfacial tension (γ) between water (saturated with ethyl acetate) and ethyl acetate (saturated with water) in the presence of LA-*g*-CS was measured using a pendant drop tensiometer (KSV 2001) as described previously (37). Measurements were carried out inside a sealed cuvette at 298 K. The results shown represent the average of three independent measurements that have a standard deviation of 0.05 mN m^{-1} or less.

Physical Stability of the Dispersions in Propellant HFAs. An exact mass of the particles were initially fed into pressure proof glass vials (68000318, West Pharmaceutical Services), and crimp-sealed with 50 μl metering valves

(EPDM Spraymiser™, 3M Inc). The glass vials and metering valves were kindly donated by West Pharmaceuticals and 3M, respectively. Subsequently, a known amount of HFA134a or HFA227 was added with the help of a manual syringe pump (HiP 50-6-15) and a home-built high pressure aerosol filler, to make a 2 mg ml^{-1} drug concentration in the propellant HFA. The dispersions were then sonicated in a low energy sonication bath (VWR, P250D, set to 180 W) for 10 min in order to break up any aggregates (24). The physical stability of the suspensions in HFAs was investigated by visually monitoring the dispersion as a function of time after mechanical energy input ceased. The stability of the formulations in HPFP was also tested.

Aerosol Characteristics. The aerosol properties of the bare and core–shell pMDI formulations were determined with an Andersen Cascade Impactor (ACI, CroPharm, Inc.) fitted with a USP induction port and operated at a flow rate of 28.3 L min^{-1}. The experiments were carried out at 298 K and 45% relative humidity. Formulations were prepared as described above. Before each test, several shots were first fired to waste. Subsequently, ten shots were released into the impactor, with an interval of 30 s between actuations. Three independent canisters were tested for each formulation. The average and standard deviation from those three independent runs are reported here. After each run, the impactor was disassembled and the valve stem, actuator, induction port and stages were rinsed thoroughly with a known volume of 0.1 N NaOH aqueous solution in the case of bare SS formulation. For the core–shell SS particles, a 0.1 N NaOH methanol solution was employed as rinse solvent instead, because the LA-*g*-CS copolymer has co-absorbance with SS in water at 243 nm. The drug content was quantified by UV spectroscopy, with a detection wavelength of 243 nm for bare SS formulation and 246 nm for the core–shell SS formulation. Bare BSA was rinsed with DI-water and quantified by UV–vis with a detection wavelength of 280 nm. BSA core–shell particles deposited on each stage were quantified by Micro-BCA assay (Pierce). To enhance the accuracy of the BCA assay analysis, 20 puffs were fired for each independent run during the analysis of the BSA core–shell formulation. The plates were placed into Petri dishes with the rinsing solvent. Samples were then drawn for quantification of SS or BSA. The effect of a spacer (Aerochamber Plus) on the aerosol characteristics was also investigated. The results obtained with the formulations proposed here are contrasted with those obtained with Ventolin HFA®. The same actuator as that of Ventolin HFA® was used in all experiments. The fine particle fraction (FPF) is defined as the percentage of drug on the respirable stages of the impactor (stage 3 to terminal filter) over the total amount of drug released into the device (from the induction port to filter).

Calu-3 and A549 Cell Culture. The cytotoxicity of the LA-*g*-CS particles was tested in vitro on the differentiated human, mucus-producing, submucosal gland carcinoma cell line Calu-3 and on human lung carcinoma cell line A549. Calu-3 cells were supplemented with 10% FBS, 100 IU ml^{-1} penicillin and 100 μg ml^{-1} streptomycin. The cells were plated in a 75 cm^2 cell culture flask and subcultured until 80% confluence was reached. The medium was changed every two days and the cells were cultivated for 14 days. The cells from passages 2–7 were used for toxicity studies. A549 cells of passage 14–18 were cultured in RPMI 1640 media supplemented with 10% FBS, 100 IU ml^{-1} penicillin and 100 μg ml^{-1} streptomycin. The cells were plated in 75 cm^2 cell and subcultured when 85% confluent.

Cytotoxicity Measurements. Calu-3 cells were cultured at a density of 1×10^4 cells $well^{-1}$ into a 96-well culture plate in DMEM supplemented with 10% FBS and 100 μg ml^{-1} penicillin and streptomycin. The cells were incubated in the medium for 24 h, and then washed with 1X PBS twice. The medium was subsequently replaced with a solution made of the core–shell particles (SS and BSA) dispersed in the same culture medium, at a particle concentration range of 0.01 to 1.5 mg ml^{-1}. Because SS, BSA, and the copolymer are water soluble, the particles quickly break down forming a homogeneous aqueous solution. The cells were incubated in this solution for 24 h. The medium containing the polymer and SS or BSA was then replaced with 100 μl of the culture medium (particle free) and 30 μl of the cell proliferation reagent MTS. The cells were allowed to incubate in this mixture for 120 min. The MTS reagent is reduced by viable cells into a formazan product that is soluble in the culture medium. The absorbance of formazan was measured at 490 nm, and its concentration directly correlated to the number of living cells in the culture (38). As a control, cells were incubated in bare (particle free) culture medium. From the absorbance ratio between the treated (with particle) and untreated cells (positive control), the cell viability was calculated (39). A similar procedure was used in the case of the A549 cell line.

RESULTS AND DISCUSSION

Design and Synthesis of the Particle Shell

There were several design parameters that guided the selection of the chemistry of the copolymer for this study. First, the chemistry of the amphiphile needed to be such that its potential toxicity was low. Based on the selected particle formation technology (emulsification–diffusion), an interfacially active polymer at the water-organic interface was required in order for the resulting morphology to be of the core–shell type (shell being the copolymer). This was required in order to modify the chemistry of the drug surface—vs. having the polymer buried within the drug particle. Several potential candidates were available as the hydrophile. However, there were significant limitations in terms of the hydrophobic/HFA-philic portion of the molecule. While the presence of a block that could be well solvated by HFA is essential, the overall solubility of the copolymer in the propellant should be minimal so that the structure of the resulting core–shell particle would be stable. Moreover, the hydrophobic block should not only be HFA-philic, but it should also interact with the organic phase used in the preparation of the core–shell particle.

Chitosan (CS) is a biocompatible and biodegradable natural polymer used in nasal spray formulations (40), and a potential candidate carrier for inhalation therapy (41). CS is a polysaccharide comprised of glucosamine and *N*-acetylglucosamine. CS is manufactured by the deacetylation of chitin,

which is the second most abundant polysaccharide in nature (13). CS can bind strongly to negatively charged cell surfaces and mucus (40). It has been determined that CS can alter the paracellular transport of drugs by directly affecting the tight junctions between the cells, due to its bioadhesive properties. For drugs with molecular weight below 10 kDa the use of CS can also lead to an improvement in drug bioavailability (40). High molecular weight CS is insoluble in neutral water which limits its application in many fields (33,42). However, its aqueous solubility can be substantially increased upon degradation to smaller oligomers (33). CS has also been shown to have low or no toxicity on respiratory cell lines that include A549 and 16HBE14o- (43–45). In our work, water-soluble oligomers of CS obtained by hydrogen peroxide degradation (33) were thus selected as the hydrophilic portion of the amphiphile.

Poly(lactide) is also biocompatible and biodegradable, and widely used in pharmaceutical applications (46–49). Low molecular weight oligo(lactide) (LA) is fairly soluble in propellant HFAs (14,50). We have used a combined computational and experimental approach to understand solvation in hydrofluoroalkane solvents (27,28). *Ab initio* calculations and chemical force microscopy results provide quantitative information on the HFA-philicity of candidate moieties (27,28). Our results showed that HFAs have significantly stronger enthalpic interactions with a fragment containing the ester group compared to its hydrogenated analog (the baseline). We have thus selected LA as the HFA-philic portion of the amphiphile.

The product of the degradation of the large MW CS with hydrogen peroxide was characterized by SEC. The determined Mn was 1,350 Da, or an average of 8.3 repeat units. The LA-*g*-CS copolymers were obtained by grafting the product of the ring-opening polymerization of lactide onto the amine and hydroxyl groups of CS (initiators), as shown in Scheme 1. The product was characterized by ^{1}H-NMR and FTIR. The NMR spectra of the CS oligomer and the LA-*g*-CS are shown in Fig. 1. Compared with the spectrum of CS oligomer, the extra peaks at 4.3 ppm and 4.9 ppm observed in the spectrum for LA-*g*-CS can be attributed to the terminal methine protons and its repeating units in the LA moiety, respectively (34,51). The peak at 1.6 ppm is attributed to the methyl protons of the LA moiety. The grafting ratio is calculated as 108% according to weight difference before and after grafting: $(W_{LA\text{-}g\text{-}CS} - W_{CS})/W_{CS}$ (34,51). The molar ratio of CS to LA is thus determined to be 2.4. By evaluating the intensity ratio of the peaks at 4.3 and 4.9 ppm on the NMR spectrum, the length of LA unit grafted onto CS was determined as 2.3, which correlates well with the gravimetric method. Similar results have also been observed in other works where oligo lactide side chains were grafted onto chitosan (34,51).

The grafting was also confirmed by FTIR, as shown in Fig. 2. Compared with the IR spectrum of degraded CS, a strong absorption peak can be observed at 1,754 cm^{-1}. This can be attributed to the carbonyl groups on the LA repeat unit (34,51). The FTIR results (compare Fig. 2a and b) also indicate no or little compositional change in the CS due to the depolymerization process.

Preparation and Characterization of the Core–shell Particles

Core–shell particles of the model polar compounds and the LA-*g*-CS copolymer were prepared by emulsification–diffusion. Salbutamol sulfate (SS), a short-acting β-agonist, was selected as the model small polar solute for this study due to its extensive use in the treatment of chronic pulmonary disorders such as asthma and COPD (52). Bovine serum albumin (BSA, ~66 kDa) was selected as the model biomolecule because it is inexpensive and easily accessible.

The emulsification–diffusion process consists in first forming an emulsion of an aqueous solution of the drug of interest (dispersed phase) into an organic phase (continuous phase) that possesses appreciable aqueous solubility (53,54). As the emulsion is subsequently diluted into an excess organic phase, water diffuses from within the emulsion droplets, thus creating a supersaturation condition (53–56). This supersaturation within the shrinking emulsion droplets leads to the formation and growth of drug nuclei that aggregate to form the particles. The drug particles are templated by the emulsion droplets, and are thus spherical and smooth. Similar results have also been observed in the preparation of insulin (57) and organic polymeric particles (53–55,58) using water and other solvents such as benzyl alcohol, propylene carbonate and triacetin. Moreover, they

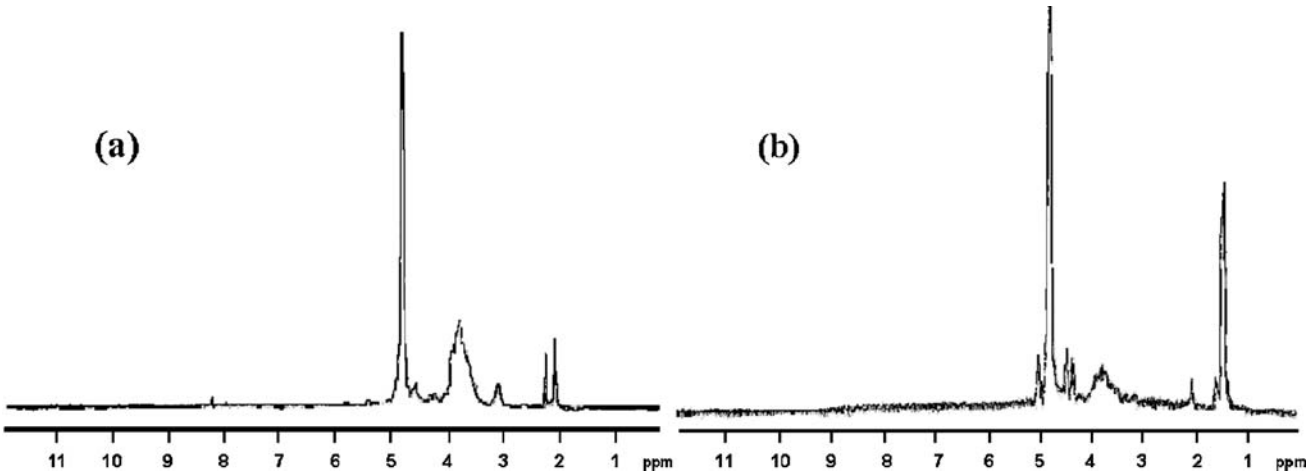

Fig. 1. NMR spectra of (**a**) chitosan oligomer, and (**b**) oligo(lactide)-grafted-chitosan.

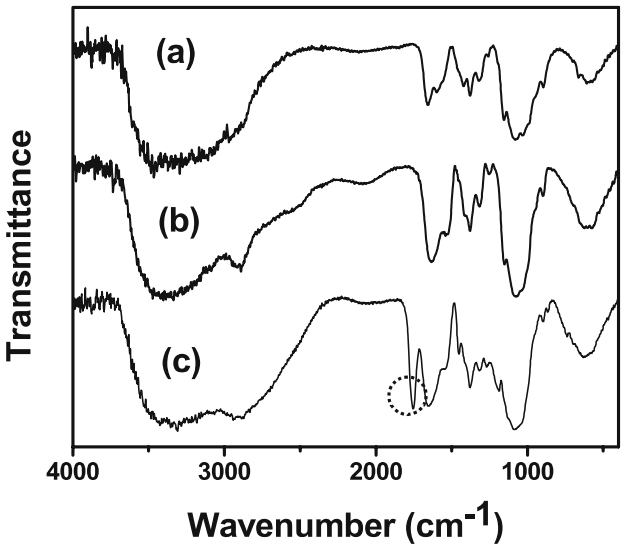

Fig. 2. FTIR spectra of (**a**) commercial chitosan; (**b**) degraded chitosan oligomer; (**c**) oligo(lactide)-grafted-chitosan.

are typically amorphous due to the time scales for particle formation (59,60).

In this work, the synthesized LA-*g*-CS copolymer was employed as a surface active agent during the emulsification process. The copolymer is expected to serve many purposes. It should help to stabilize the water–oil interface (prevent coalescence of the droplets), thus reducing the polydispersity of the particles. If well-balanced, the amphiphile should also help reduce the tension of the water–oil interface, which will in turn allow the formation of smaller emulsion droplets (drug particles) for the same energy input. Most importantly, the use of the copolymer should provide for a means of modifying the chemistry of the drug surface, thus enhancing its dispersability in propellant HFAs.

The interfacial activity of the LA-*g*-CS copolymer as a function of its concentration was investigated at the water–oil (ethyl acetate) interface, and the results are shown in Fig. 3. Since no experimental density values of the mutually saturated phases are available in the literature, we use the density of pure water and ethyl acetate to calculate γ, once the droplet profile was digitized (37). While this assumption might affect the absolute values of the reported tension, the relative (trend) effect of the copolymer on the tension is expected to remain unchanged. The results show that the LA-*g*-CS copolymer is indeed capable of reducing the tension of the water–ethyl acetate interface from 6.3 mN m^{-1} at 298 K for the bare interface, down to about 2.3 mN m^{-1}. The interfacial tension seems to level off at an LA-*g*-CS concentration of about 12 mg ml^{-1}. Based on this finding we decided to use a concentration slightly higher than that for the preparation of the core–shell particles.

Particles of an aqueous solution of pure LA-*g*-CS copolymer, of the copolymer in the presence of SS, and with the copolymer in the presence of BSA were prepared as discussed above. The concentration of the polar solute and the copolymer in the aqueous phase was kept constant at 31 and 15 mg ml^{-1}, respectively. SEM images of the particles are shown in Fig. 4. The micrographs obtained for particles with pure LA-*g*-CS copolymer (no drug) indicate the formation of hollow capsules. The particles are fairly polydisperse, with a size range of approximately 0.5 to 7 μm. While the gold plating for the SEM analysis distorts somewhat the shape of the particles, and also induces the collapse in some others, smooth and approximately spherical particles can be seen in Fig. 4a. These results confirm that the copolymer is not only interfacially active, but also tends to reside/migrate to the interface during the emulsification–diffusion process. The morphology of the LA-*g*-CS coated SS and BSA core–shell particles prepared are shown in Fig. 4b and c. TEM images (insets in Fig. 4b and c) clearly evidence the core–shell morphology of the SS and BSA particles formed, with a large fraction being segregated to the particle surface. While it is likely that some copolymer will be trapped within the core of the particle, the overall distribution is not important—the key point is that enough of the copolymer remains/reaches the particle surface in order to reduce the cohesive forces (as shown by CPM in the following section), thus improving the overall physical stability and the aerosol characteristics of the formulation. The SEM images indicate that the particles are smooth and spherical. Particles with sizes ranging from 0.5 to 3.5 μm are observed for the BSA spheres, while significantly smaller and less polydisperse spheres are seen for the SS core–shell system. This difference can be loosely attributed to a likely increase in the viscosity of the internal phase in the presence of BSA (55). A slightly lower temperature for the BSA system can also impact (reduce) the viscosity and thus particle size and distribution (55,58).

We expect the proposed methodology to translate well to other small polar solutes that are well solvated by water; i.e., with low interfacial activity at the water-organic solvent of interest. By the same token, we anticipate that due to the presence of hydrophobic patches, different biomolecules will possess different degrees of interfacial activity and may thus yield different results. This problem can be circumvented by either the selection of an appropriate organic phase (55,57), and/or the use of diluents in the aqueous phase (57). Systems with high density of interfacially active species will also tend to reduce unfavorable co-adsorption effects by preventing the drug molecules to partition as strongly to the interface.

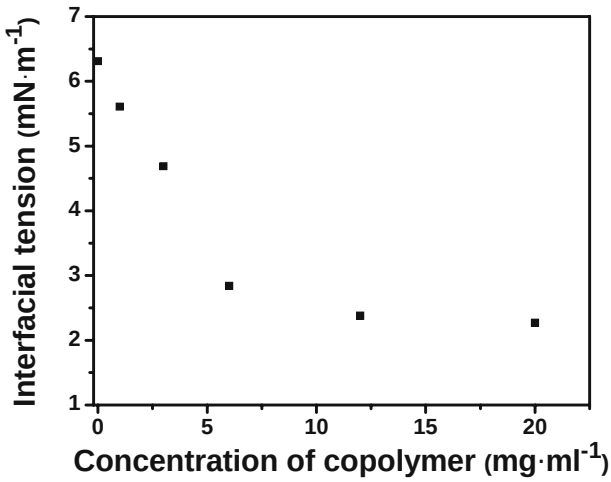

Fig. 3. Activity of the oligo(lactide)-*g*-chitosan at the water–ethyl acetate interface.

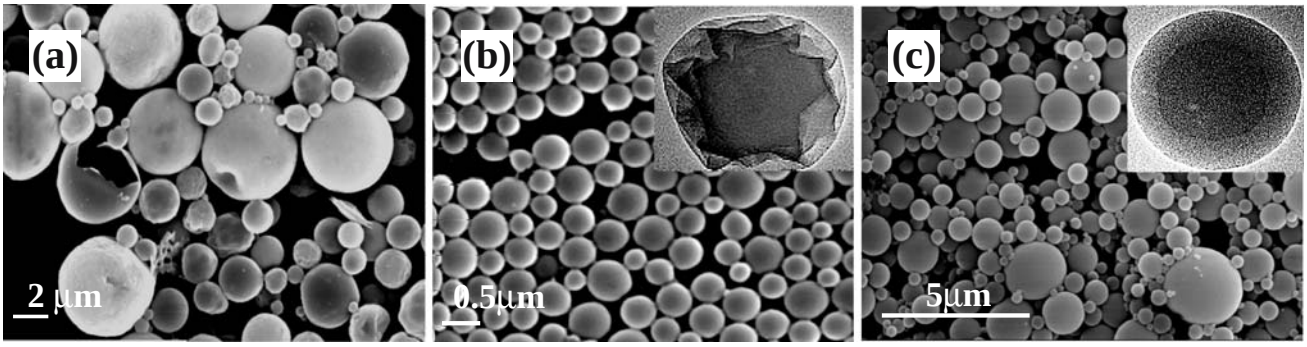

Fig. 4. SEM images of particles formed by emulsification–diffusion at 0.8:19 water to ethyl acetate volume ratio (W:Ac, ml) (**a**) hollow capsules of pure oligo(lactide)-*g*-chitosan prepared at 295 K, (**b**) SS core–shell particles prepared at 311 K; (*inset*) TEM image: the drug core appears dark and the polymeric shell brighter; (**c**) BSA core–shell particles prepared at 283 K; (inset) TEM image where the core appears dark and the polymeric shell brighter.

Cohesive Interactions from Colloidal Probe Microscopy (CPM)

The effect of the surface modification on the cohesive interactions was assessed by Colloidal Probe Microscopy (CPM) (35). CPM is a modified version of the AFM technique where the force of interaction between a particle attached to an AFM cantilever and that on a substrate/or a substrate is measured with high accuracy. CPM has been used to investigate several systems of relevance in pharmaceutical applications (35), including drugs suitable for inhalation therapy in vehicles such as DPIs and pMDIs (14,15,31,32). In this work, the interaction between core–shell particles (particles with the surface modified by the LA-*g*-CS copolymer) was determined by CPM in liquid HPFP, a mimic to HFA propellants (29–31,36,37), at 298 K.

Figure 5a is an SEM image of an AFM cantilever modified with a single SS particle. A similar micrograph was observed for the core–shell particle (not shown). The cohesion force (F_{co}) results plotted as the F_{co} frequency vs. cohesion force are shown in Fig. 5b. Average cohesion curves are shown in the inset.

The F_{co} for the SS core–shell particles, which varies from 0 to a maximum of 0.08 nN—approximately 18% of the force curves show zero F_{co}, is observed to be significantly lower than that for bare SS particles of similar size—1.36±1.80 nN. The same trend was observed for bare BSA and BSA core–shell particles, as shown in Fig. 5c. F_{co} was reduced from 2.90±0.70 nN (bare BSA particles) down to 0.32±0.05 nN for the core–shell BSA particles. Besides differences in chemistry between the SS and BSA particles, the increase in F_{co} observed in the BSA systems might also be attributed to a variation (increase) in contact area. Large variations in contact area, and thus in F_{co}, are typically observed even for probes of the same chemistry (30–32,61). The presence of (interfacially active) biomolecules trapped at the interface during the particle formation process might also contribute to an increase in F_{co}. The much lower F_{co} observed for the core–shell particles compared with the corresponding bare particles suggests that the LA-*g*-CS shell is capable of screening the cohesive forces between the drug particles.

The CPM technique is certainly more demanding than sedimentation rate experiments both in terms of time for preparation of the probe and the actual F_{co} measurements, and also with regards to the skill level required to perform the experiments. However, CPM is considered a very powerful screening technique because the information on single particle–particle interactions is not available from bulk physical stability studies. Such results allow us to more directly correlate the aerosol characteristics of the formulations with the effect of additives or particle engineering approaches—vs. other formulation parameters as for example the physical characteristics of the device. In this case, CPM results also serve to confirm the proposed mechanism for the formation of the core–shell particles where the copolymer is seen to become the particle shell, with the outer most part being LA, the HFA-philic group. Bulk physical stability in the propellant HFAs are, however, still required in order to assess the validity and potential to extrapolate the CPM results obtained in the mimicking HPFP solvent to the actual hydrofluoroalkane propellants (18,31). Sedimentation rate experiments are, therefore, discussed below.

Dispersion Stability of the Core–shell Formulations in HFA Propellants

Sedimentation rate experiments of the bare and core–shell SS and BSA particles were performed in HFA134a and HFA227 at 298 K and saturation pressure of the propellant. The results for HFA227 are summarized in Fig. 6. We can see from Fig. 6a that, as expected, bare SS spheres obtained from emulsification–diffusion had poor stability in the hydrofluoroalkane propellant. Creaming of the particles (less dense than HFA227) started taking place in just a few seconds after mechanical input used for dispersing the particles stopped. The surface modification of the drug particles by the formation of the LA-*g*-CS copolymer shell generates suspensions with excellent colloidal stability in HFA227, as shown in Fig. 6b. The stability of bare BSA and BSA core–shell particles are shown in Fig. 6c and d. While bare BSA particles cream out faster than the bare SS formulation, the stability of the core–shell BSA formulation is similar to that of core–shell SS particles. Similar behavior was observed in HFPF at 298 K and ambient pressure. The results are in agreement with the F_{co} from CPM measurements in HPFP, and indicate that indeed HPFP is a good mimicking solvent to HFA227. Even after three months of storage at ambient

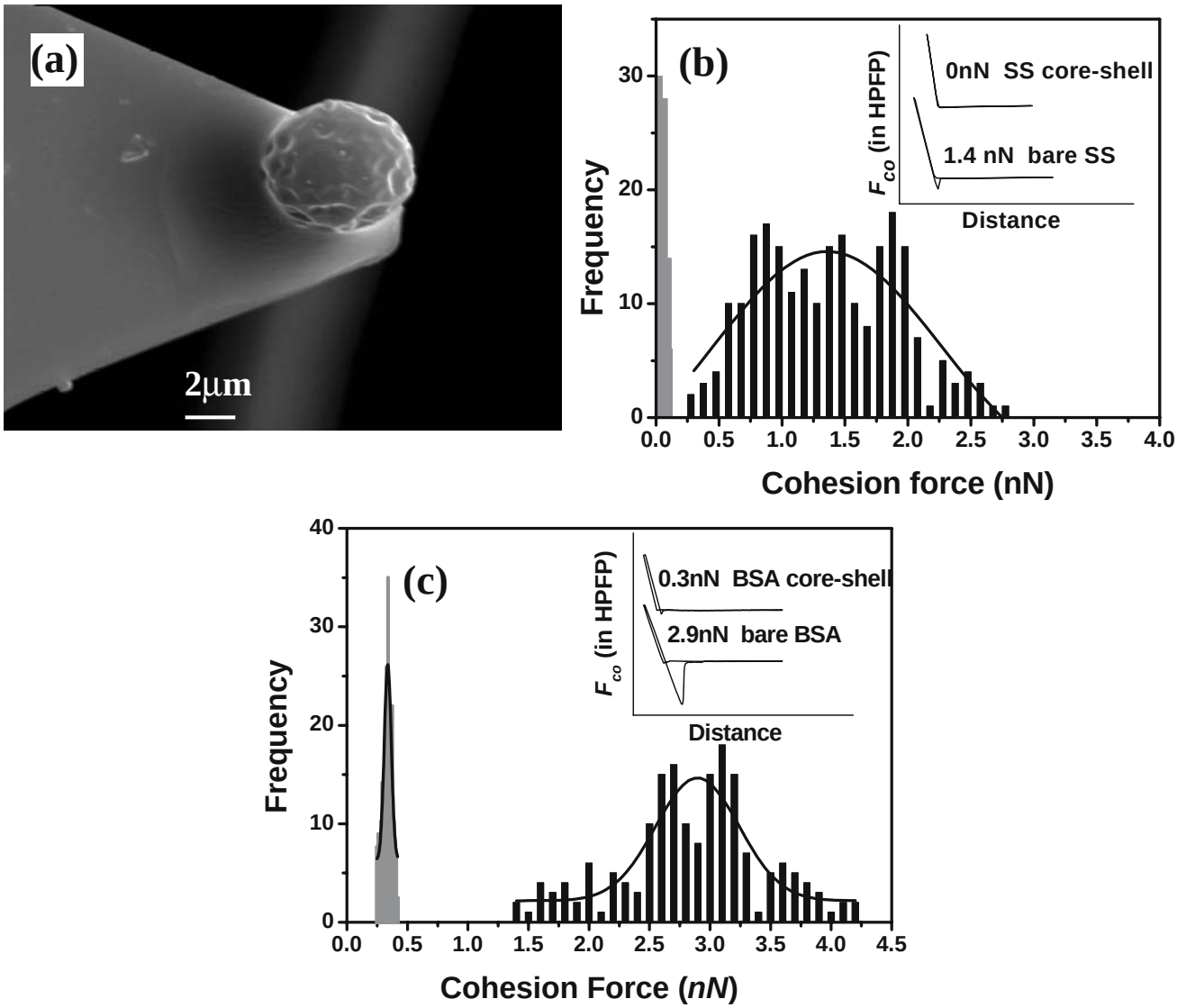

Fig. 5. (**a**) SEM image of a bare salbutamol sulfate (SS) sphere modified AFM cantilever. (**b**) Cohesion force (F_{co}) histogram between bare SS (distribution to the *right* of the diagram) and oligo(lactide)-*g*-chitosan SS core–shell spheres (distribution to the left of the diagram). (**c**) Cohesion force (F_{co}) histogram between bare BSA (distribution to the *right* of the diagram) and oligo(lactide)-*g*-chitosan BSA core–shell spheres (distribution to the *left* of the diagram). Determined in HPFP at 298 K. *Inset*: average force curves for bare-SS/BSA and SS/BSA core–shell particles. The Gaussian fits to the histogram are shown.

conditions, the SS core–shell formulations in HFA227 can be easily resuspended by manual agitation, thus indicating that no irreversible flocculation occurs. A similar behavior has been seen for BSA core–shell particles, with an ongoing test that has lasted for approximately 2 weeks so far. The same is not true for bare SS particles.

The stability of the core–shell particles in HFA134a, on the other hand, was very poor. According to our previous work, HPFP seems indeed to be a more appropriate mimicking solvent to HFA227 than HFA134a, especially in terms of solvation power (28). The difference in the nature of the interaction between HFA227 and HFA134a with different chemistries has not yet been addressed at the microscopic level. Through the decomposition of the binding energy from *ab intio* calculations we expect to identify the relative contributions (e.g. dispersive vs. electrostatic) to the overall energy. This will be part of a forthcoming publication.

Aerosol Performance of the Core–shell Formulation

Anderson Cascade Impactor (ACI) is widely used in simulating drug lung deposition in-vitro.(14,15) ACI usually contains eight stages with decreasing orifice sizes, which simulate the various parts of the human respiratory system (14,15). By pulling vacuum through the ACI at a constant flow rate, particles are deposited on the different stages. The amount of drug deposited on each stage can be quantified by different analytical techniques, thus providing information on the aerosol characteristics of the formulation such as mass mean aerodynamic diameter (MMAD), geometric standard deviation (GSD) (62,63), and fine particle fraction (FPF). The aerosol performance of the LA-*g*-CS SS and BSA core–shell formulations in HFA227, as determined with the ACI are shown in Table I. The results for a commercial SS formulation (Ventolin HFA®) and the formulation contain-

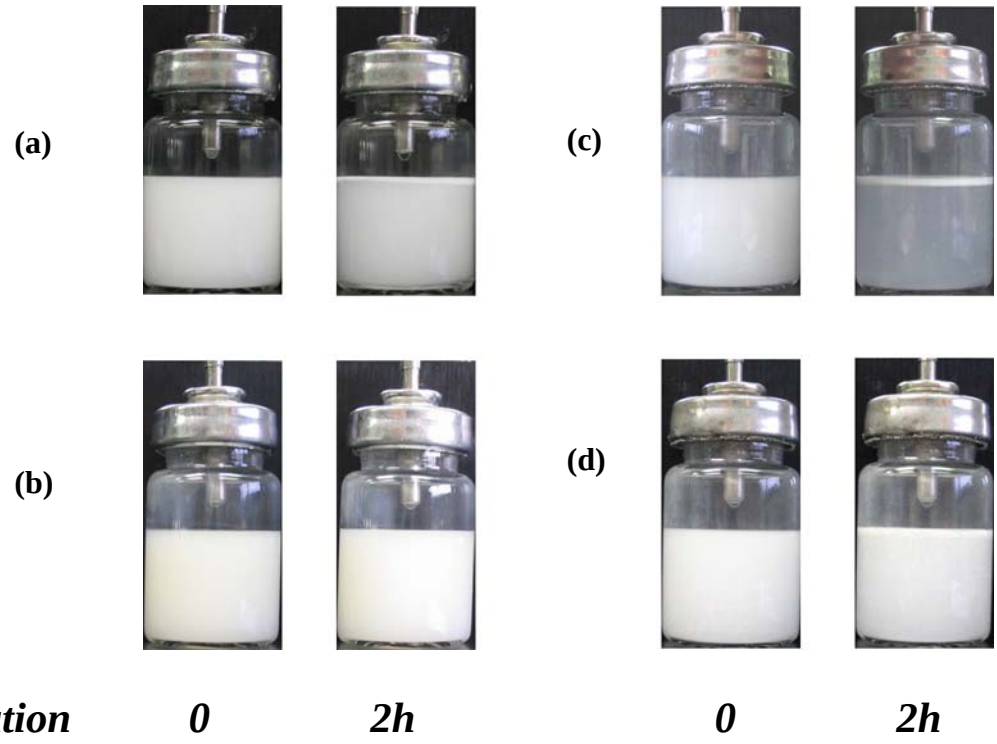

Fig. 6. Dispersion stability of SS spheres in HFA227 at 298 K and saturation pressure of the propellant. (**a**) Bare SS particles; (**b**) oligo(lactide)-*g*-chitosan SS core–shell particles; (**c**) bare BSA particles; and (**d**) oligo(lactide)-*g*-chitosan BSA core–shell particles.

ing bare SS and bare BSA spheres are also listed in Table I for comparison. The effect of the spacer on the characteristics of the aerosol is also investigated.

A summary of the results is shown in Fig. 7a, b and c. The amount retained at each stage of the ACI is reported as dosage percentage of the total amount of drug delivered from the pMDI. Plotting the results in terms of % allows us to directly compare the different formulations. The aerosol performance of the LA-*g*-CS core–shell SS formulation is significantly improved compared to both the commercial formulation and the bare SS particles formed using the emulsification–diffusion technique. The FPF without spacer is enhanced by 28% compared to the commercial Ventolin HFA®, and 39% in compared to the bare SS formulation, reaching a value of 74.4%. Particular improvement is observed in the amount of drug retained in stages 5, 6 and 7, clearly indicating the potential of the proposed formulation for the enhanced delivery to the deep lungs. The FPF for the core–shell formulation in the presence of a spacer is further improved, going up to 85.8%. The core–shell formulation produced aerosols with smaller MMAD (2.0 μm) than both commercial and bare SS formulations. After 3 months storage at ambient conditions the FPF and MMAD of core–shell formulation remain unchanged, indicating good storage stability. A significant improvement in FPF from 40.3% to 68.1% was also observed for BSA core–shell formulation compared to the bare BSA formulation. The somewhat lower values for the FPF in the BSA core–shell formulation when compared to the SS system might be attributed to differences in size and size distribution of the particles and/or the slight increase in the cohesive forces as observed by CPM. These results correlate well with the CPM and physical stability tests that show that SS core–shell particles have reduced cohesive interactions and improved suspension stability. It is important to note that, unlike the optimized commercial formulation, no optimization was attempted for the core–shell formulation being discussed here (e.g. tailor particle size, size distribution, searching for optimal valve geometry, etc.), suggesting that even greater improvement can be achieved with the proposed formulation in terms of aerosol characteristics.

Cytotoxicity of the Core–shell Particles

The determination of cell viability is a common method to evaluate the in vitro cytotoxicity of biomaterials. Calu-3 cells belong to the airway epithelium and are known to form tight monolayers and secrete components of mucus and surfactant (64). A549 cells are alveolar type II cells (64). Along with the A549 cell line, Calu-3 cells have been extensively used for evaluating the efficacy and safety of particulate pulmonary drug delivery systems (43–45). We have, therefore, selected both Calu-3 and A549 cells to study the cytotoxicity of the proposed formulation, and in particular of the LA-*g*-CS copolymer.

Figures 8a and b show the cell viability results for the hollow (pure) LA-*g*-CS particles and the core–shell formulations on A549 and Calu-3 cell lines, respectively. When assayed independently, neither of the formulation components reduced the cell viability of either the A549 or the Calu-3 cell lines to the extent of 50% inhibitory concentration. Among the three formulations tested, the lowest cell

Table I. Aerodynamic Properties of Various SS and BSA Formulations as Probed by the ACI Test

Stages	Ventolin HFA		Bare-SS		SS Core–shell		Bare-BSA	BSA Core–shell
	HFA134a (μg±s.d., n=3) 10×puff		HFA227 (μg±s.d., n=3) 10×puff		HFA227 (μg±s.d., n=3) 10×puff		HFA227 (μg±s.d., n=3) 10×puff	HFA227 (μg±s.d., n=3) 20×puff
	No Spacer	With Spacer	No Spacer	With Spacer	No Spacer	With Spacer	No Spacer	No Spacer
AC	163.9±10.2	115.7±12.5	157.4±16.5	142.2±17.2	92.7±7.7	46.2±3.4	105.0±9.8	151.9±10.3
SP	N/A	332.6±20.2	N/A	237.7±22.0	N/A	94.4±8.3	N/A	N/A
IP	459.5±23.1	104.6±13.4	296.4±21.5	59.3±5.5	103.1±8.7	35.3±1.9	253.8±15.4	322.8±19.9
Stage 0 (9.0–10.0 μm)	16.3±1.0	12.2±2.1	28.9±4.2	34.6±3.2	21.8±2.4	18.9±1.0	56.3±3.4	54.2±3.7
Stage 1 (5.8–9.0 μm)	18.3±1.6	16.6±1.2	53.5±5.4	54.3±4.2	32.2±1.7	26.5±2.9	61.5±4.9	62.5±2.9
Stage 2 (4.7–5.8 μm)	24.2±1.5	22.8±3.4	76.4±6.6	73.9±5.7	40.6±2.6	26.7±2.7	87.1±7.0	124.0±10.1
Stage 3 (3.3–4.7 μm)	89.6±7.6	95.3±4.6	113.1±9.8	115.1±10.4	57.2±4.5	64.8±4.8	94.7±8.9	212.5±14.5
Stage 4 (2.1–3.3 μm)	217.5±12.4	281.9±14.9	83.5±7.8	83.6±6.8	170.0±10.4	197.4±15.6	84.5±6.5	488.1±30.4
Stage 5 (1.1–2.1 μm)	131.9±10.1	163.9±9.4	33.3±2.1	38.0±1.7	217.8±10.9	246.5±13.3	64.0±2.9	328.9±21.1
Stage 6 (0.7–1.1 μm)	18.8±1.2	21.2±1.1	13.0±1.0	10.1±1.3	80.0±5.7	77.4±4.8	30.7±2.3	106.1±9.8
Stage 7 (0.4–0.7 μm)	6.0±0.6	8.4±1.0	8.4±1.1	9.1±1.0	54.2±3.1	41.6±2.4	28.2±2.1	41.6±3.6
Filter (0–0.4 μm)	3.5±1.1	5.7±2.1	5.2±1.8	7.5±1.1	26.2±2.2	18.2±2.5	15.4±1.8	18.5±2.0
Single puff dose	118.2±5.8	121.1±4.9	88.7±5.4	89.1±5.6	90.6±2.5	91.7±3.0	85.4±4.1	93.4±3.0
FPF (%)	45.9±2.4	78.7±2.9	35.1±2.6	54.2±2.8	74.4±1.6	85.8±1.4	40.3±1.8	68.1±2.1
MMAD (μm)	2.5±0.1	2.3±0.1	3.7±0.2	3.7±0.2	2.0±0.1	2.0±0.1	3.1±0.2	2.3±0.1
GSD (μm)	1.9±0.1	1.8±0.1	2.2±0.1	2.2±0.2	2.3±0.2	2.1±0.1	2.6±0.2	2.1±0.1

AC, IP, SP and F refer to actuator and valve stem, induction port, spacer and filter respectively.
(μg±s.d., n=3) = represent mean mass (μg) and the standard deviation (± s.d.) for three batches (n=3).

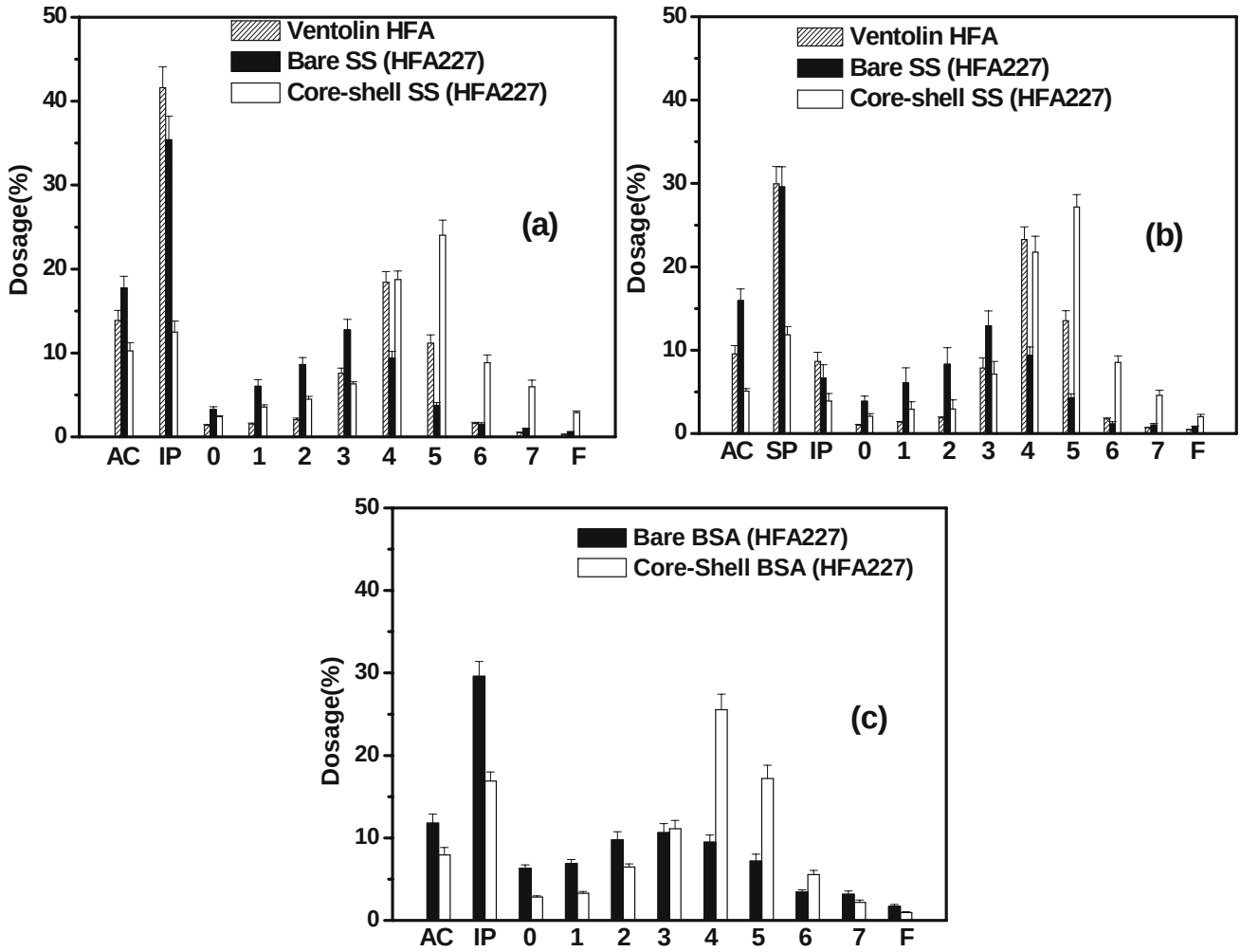

Fig. 7. Aerodynamic characteristics of (**a**) Ventolin HFA®, and bare SS, and oligo(lactide)-*g*-chitosan SS core–shell formulations without the spacer; and (**b**) with the spacer; (**c**) bare BSA, and oligo(lactide)-*g*-chitosan BSA core–shell formulations without the spacer. Formulations in HFA227 at 298 K and 2 mg ml^{-1} particle concentration. AC, IP, SP and F refer to actuator and valve stem, induction port, spacer and filter respectively.

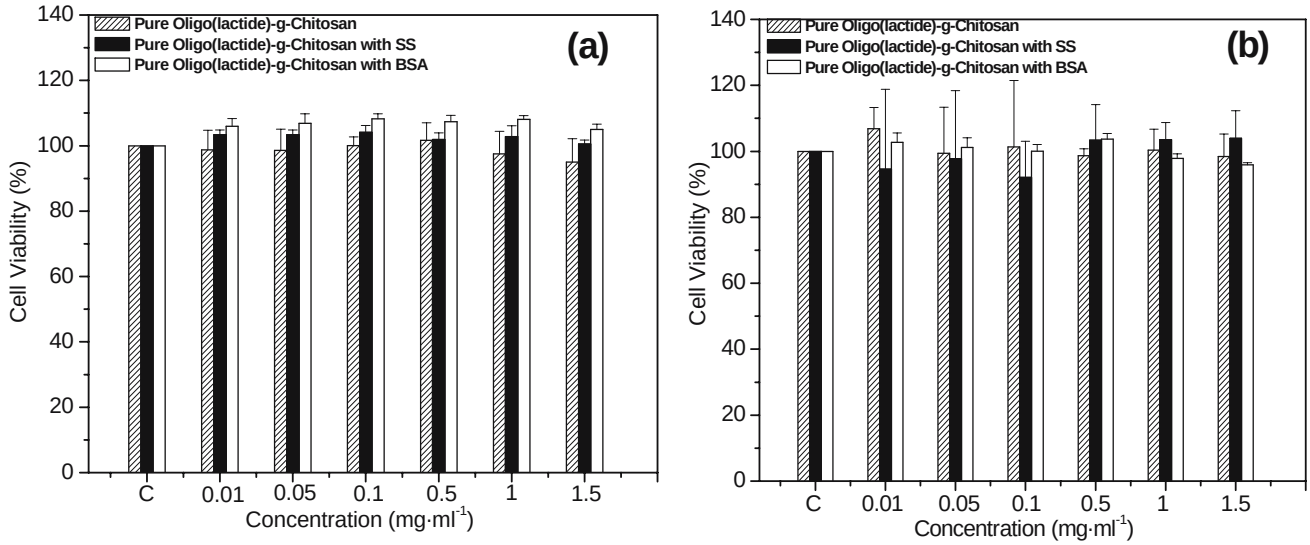

Fig. 8. The effect of hollow oligo(lactide)-*g*-chitosan particles, core–shell SS and BSA particles (where shell is the oligo(lactide)-*g*-chitosan copolymer) on mitochondrial-dehydrogenase activity of (**a**) A549 and (**b**) Calu-3 cells. The results represent the average of three independent experiments.

viability (in comparison to the untreated control) was 92% for the pure LA-*g*-CS and 95% for the SS core–shell particles on the A549 cells. The lowest cell viability in Calu-3 cells was 92% in case of the SS core–shell formulation. It is interesting to note that the BSA encapsulated core–shell particles did not induce any cell-kill within this concentration range on the A549 cell line. However, a reduction in the cell viability was observed in case of the Calu-3 cells for the same system. These results corroborate a number of previous studies that have also indicated CS or CS-based formulations to be fairly non-toxic on lung cells at moderate to high concentrations (43,44).

CONCLUSIONS

In this work we demonstrate the applicability of novel core–shell particles in the development of stable dispersions of both small polar drugs and biomolecules in hydrofluoroalkane (HFA) propellants. The idea is to modify the surface chemistry of the drug particles with an HFA-philic moiety capable of screening the cohesive forces responsible for the physical instability in suspension-based formulations. Core–shell particles with a model small polar drug (salbutamol sulfate) and a model biomolecule (BSA) were prepared by emulsification diffusion. The particle shell consisted in oligo(lactide) (LA) grafts attached onto a short (degraded) chitosan (CS) backbone. The copolymer with the biodegradable and biocompatible blocks was carefully designed to be interfacially active at the water–ethyl acetate interface, thus producing the core–shell morphology during emulsification diffusion, and at the same time to incorporate an HFA-philic branch (LA) that could enhance the stability of the particles in HFAs. Colloidal probe microscopy (CPM) results obtained in a mimicking HFA propellant indicate that the cohesive forces between drug particles is significantly reduced to nearly zero upon the addition of the shell around the drug particle. The CPM results correlate well with the bulk physical stability in HFA277. Stable core–shell dispersions also have significantly larger fine particle fractions compared to bare particles (baseline), and in the case of SS, the aerosol characteristics of the core–shell formulation was also significantly improved compared to a commercial pMDI formulation. Cytotoxicity analysis demonstrated that the synthesized LA-*g*-CS copolymer has no toxic effect on lung alveolar epithelial A549 or airway epithelial Calu-3 cells.

ACKNOWLEDGEMENTS

L.W. acknowledges Wayne State University (WSU) for a Ph.D. assistantship. The authors would also like to acknowledge Solvay Fluor und Derivate GmbH & Co., Hannover—Germany, for the propellant HFAs; West Pharmaceuticals and 3M, for the glass vials and metering valves, respectively; Dr. Verani's group (Department of Chemistry at WSU), Dr. Oupicky's group (College of Pharmacy at WSU), and Dr. Sujatha Kannan's group (Med School at WSU) for providing access to the FTIR, GPC and plate reader, and the A549 cell line, respectively; and financial support from the Office of the VP for Research at Wayne State University, through a Nano@Wayne grant, and from the National Science Foundation through an NSF-CBET grant no. 0553537.

REFERENCES

1. R. U. Agu, M. I. Ugwoke, M. Armand, R. Kinget, and N. Verbeke. The lung as a route for systemic delivery of therapeutic proteins and peptides. *Respir. Res.* **2**:198–209 (2001).
2. M. Bivas-Benita, T. H. M. Ottenhoff, H. E. Junginger, and G. Borchard. Pulmonary DNA vaccination: concepts, possibilities and perspectives. *J. Control. Release* **107**:1–29 (2005).
3. L. R. Brown. Commercial challenges of protein drug delivery. *Expert. Opin. Drug Delivery* **2**:29–42 (2005).
4. S. A. Cryan. Carrier-based strategies for targeting protein and peptide drugs to the lungs. *AAPS J.* **7**:20–41 (2005).
5. B. L. Laube. The expanding role of aerosols in systemic drug delivery, gene therapy, and vaccination. *Respir. Care.* **50**:1161–1176 (2005).
6. D. T. O'Hagan and R. Rappuoli. Novel approaches to vaccine delivery. *Pharm. Res.* **21**:1519–1530 (2004).
7. J. S. Patton. Mechanisms of macromolecule absorption by the lungs. *Adv. Drug Delivery Rev.* **19**:3–36 (1996).
8. H. M. Courrier, N. Butz, and T. F. Vandamme. Pulmonary drug delivery system: recent developments and prospects. *Crit. Rev. Ther. Drug Carrier Syst.* **19**:425–498 (2002).
9. D. K. Malik, S. Baboota, A. Ahuja, S. Hasan, and J. Ali. Recent advances in protein and peptide drug delivery systems. *Current Drug Delivery* **4**:141–151 (2007).
10. D. R. Owens, B. Zinman, and G. Bolli. Alternative routes of insulin delivery. *Diabetic Med.* **20**:886–898 (2003).
11. Y. Berthiaume, K. H. Albertine, M. Grody, G. Fick, and M. A. Matthay. Protein clearance from the air spaces and lungs of unanesthetized sheep over 144 h. *J. Appl. Physiol.* **67**:1887–1897 (1989).
12. R. H. Hastings, M. Grady, T. Sakuma, and M. A. Matthay. Clearance of different-sized proteins from the alveolar space in humans and rabbits. *J. Appl. Physiol.* **73**:1310–1316 (1992).
13. S. S. Davis. Delivery of peptide and non-peptide drugs through the respiratory tract. *Pharm Sci Technol To.* **2**:450–456 (1999).
14. P. Rogueda. Novel hydrofluoroalkane suspension formulations for respiratory drug delivery. *Expert. Opin. Drug Delivery.* **2**:625–638 (2005).
15. M. J. Telko and A. J. Hickey. Dry powder inhaler formulation. *Respir. Care* **50**:1209–1227 (2005).
16. K. J. McDonald and G. P. Martin. Transition to CFC-free metered dose inhalers—into the new millennium. *Int. J. Pharm.* **201**:89–107 (2000).
17. H. D. C. Smyth. Propellant-driven metered-dose inhalers for pulmonary drug delivery. *Expert. Opin. Drug Delivery.* **2**:53–74 (2005).
18. D. Traini, P. M. Young, P. Rogueda, and R. Price. In vitro investigation of drug particulates interactions and aerosol performance of pressurized metered dose inhalers. *Pharm. Res.* **24**:125–135 (2007).
19. C. Vervaet and P. R. Byron. Drug-surfactant-propellant interactions in HFA-formulations. *Int. J. Pharm.* **186**:13–30 (1999).
20. L. A. Dellamary, T. E. Tarara, D. J. Smith, C. H. Woelk, A. Adractas, M. L. Costello, H. Gill, and J. G. Weers. Hollow porous particles in metered dose inhalers. *Pharm. Res.* **17**:168–174 (2000).
21. D. A. Edwards, J. Hanes, G. Caponetti, J. Hrkach, A. Ben-Jebria, M. L. Eskew, J. Mintzes, D. Deaver, N. Lotan, and R. Langer. Large porous particles for pulmonary drug delivery. *Science.* **276**:1868–1871 (1997).
22. S. A. Jones, G. P. Martin, and M. B. Brown. Stabilization of deoxyribonuclease in hydrofluoroalkanes using miscible vinyl polymers. *J. Control. Release* **115**:1–8 (2006).
23. Y.-H. Liao, M. B. Brown, S. A. Jones, T. Nazir, and G. P. Martin. The effects of polyvinyl alcohol on the in vitro stability and delivery of spray-dried protein particles from surfactant-free HFA 134a-based pressurised metered dose inhalers. *Int. J. Pharm.* **304**:29–39 (2005).
24. T. E. Tarara, M. S. Hartman, H. Gill, A. A. Kennedy, and J. G. Weers. Characterization of suspension-based metered dose inhaler formulations composed of spray-dried budesonide microcrystals dispersed in HFA-134a. *Pharm. Res.* **21**:1607–1614 (2004).

25. D. A. Edwards, A. Ben-Jebria, and R. Langer. Recent advances in pulmonary drug delivery using large, porous inhaled particles. *J. Appl. Physiol.* **85**:379–385 (1998).
26. D. H. Napper. *Polymeric Stabilization of Colloidal Dispersions*, Academic Press, Orlando, 1983.
27. L. Wu, R. P. S. Peguin, and S. R. P. da Rocha. Understanding solvation in hydrofluoroalkanes: ab initio calculations and chemical force microscopy. *J Phys Chem B* **111**:8096–8104 (2007).
28. R. P. S. Peguin, L. Wu, and S. R. P. da Rocha. The Ester Group: how hydrofluoroalkane-philic is it. *Langmuir.* **23**:8291–8194 (2007).
29. R. Ashayer, P. F. Luckham, S. Manimaaran, and P. Rogueda. Investigation of the molecular interactions in a pMDI formulation by atomic force microscopy. *Colloids Surf, A* **21**:533–543 (2004).
30. D. Traini, P. Rogueda, P. M. Young, and R. Price. Surface energy and interparticle forces correlations in model pMDI formulations. *Pharm. Res.* **22**:816–825 (2005).
31. D. Traini, P. M. Young, P. Rogueda, and R. Price. Investigation into the influence of polymeric stabilizing excipients on interparticulate forces in pressurised metered dose inhalers. *Int. J. Pharm.* **320**:58–63 (2006).
32. P. M. Young, R. Price, D. Lewis, S. Edge, and D. Traini. Under pressure: predicting pressurized metered dose inhaler interactions using the atomic force microscope. *J Colloid Interface Sci* **261**:298–302 (2003).
33. F. Tian, Y. Liu, K. Hu, and B. Zhao. The depolymerization mechanism of chitosan by hydrogen peroxide. *J. Mater Sci.* **38**:4709–4712 (2003).
34. Y. Liu, F. Tian, and K. A. Hu. Synthesis and characterization of a brush-like copolymer of polylactide grafted onto chitosan. *Carbohydr. Res.* **339**:845–851 (2004).
35. H.-J. Butt, B. Cappella, and M. Kappl. Force measurements with the atomic force microscope: Technique, interpretation and applications. *Surf. Sci. Rep.* **59**:1–152 (2005).
36. P. G. A. Rogueda. HPFP, a model propellant for pMDIs. *Drug Dev. Ind. Pharm.* **29**:39–49 (2003).
37. P. Selvam, R. P. S. Peguin, U. Chokshi, and S. R. P. Rochada. Surfactant design for the 1,1,1,2-tetrafluoroethane-water interface: ab initio calculations and in situ high-pressure tensiometry. *Langmuir.* **22**:8675–8683 (2006).
38. T. L. Riss and R. A. Moravec. Comparison of MTT, XTT and a novel tetrazolium compound MTS form in vitro proliferation and chemosensitivity assays. *Mol. Biol. Cell (Suppl).* **3**:184a, 1992 (1992).
39. M. Amidi, S. Romeijn, G. Borchard, H. E. Junginger, W. E. Hennink, and W. Jiskoot. Preparation and characterization of protein-loaded *N*-trimethyl chitosan nanoparticles as nasal delivery system. *J. Controlled Release* **111**:107–116 (2006).
40. L. Illum, I. Jabbal-Gill, M. Hinchcliffe, A. N. Fisher, and S. S. Davis. Chitosan as a novel nasal delivery system for vaccines. *Adv. Drug Delivery Rev.* **51**:81–96 (2001).
41. R. O. Williams III, M. K. Barron, M. Jose Alonso, and C. Remunan-Lopez. Investigation of a pMDI system containing chitosan microspheres and P134a. *Int. J. Pharm.* **174**:209–222 (1998).
42. S. Lu, X. Song, D. Cao, Y. Chen, and K. Yao. Preparation of water-soluble chitosan. *J. Appl. Polym. Sci.* **91**:3497–3503 (2004).
43. A. Grenha, C. I. Grainger, L. A. Dailey, B. Seijo, G. P. Martin, C. Remunan-Lopez, and B. Forbes. Chitosan nanoparticles are compatible with respiratory epithelial cells in vitro. *Eur. J. Pharm. Sci.* **31**:73–84 (2007).
44. B. I. Florea, M. Thanou, H. E. Junginger, and G. Borchard. Enhancement of bronchial octreotide absorption by chitosan and *N*-trimethyl chitosan shows linear in vitro/in vivo correlation. *J. Control Release.* **110**:353–361 (2006).
45. M. Huang, E. Khor, and L.-Y. Lim. Uptake and cytotoxicity of chitosan molecules and nanoparticles: effects of molecular weight and degree of deacetylation. *Pharm. Res.* **21**:344–353 (2004).
46. M. F. Zambaux, F. G. Bonneaux, R. E. Dellacherie, and C. Vigneron. Preparation and characterization of protein C-loaded PLA nanoparticles. *J. Controlled Release.* **60**:179–188 (1999).
47. S. A. Hagan, S. E. Dunn, M. C. Garnett, M. C. Davies, L. Illum, and S. S. Davis. PLA-PEG micelles—a novel drug delivery system. *Proc. Intern. Symp. Controlled Release Bioact. Mater.* **22nd**:194–195 (1995).
48. M. A. Vandelli, B. Ruozi, and F. Forni. PLA microparticles for the prolonged release of nimesulide: effect of preparative variables. *STP Pharma Sci.* **9**:567–572 (1999).
49. A. Vila, A. Sanchez, C. Evora, I. Soriano, J. L. Vila Jato, and M. J. Alonso. PEG-PLA nanoparticles as carriers for nasal vaccine delivery. *J. Aerosol. Med.* **17**:174–185 (2004).
50. J. S. Stefely, D. C. Duan, P. B. Myrdal, D. L. Ross, D. W. Schultz, and C. L. Leach. Desing and utility of a novel class of biocompatible excipients for HFA-based MDIs. *Respir. Drug Delivery* **VII**:83–90 (2000).
51. G. E. Luckachan and C. K. S. Pillai. Chitosan/oligo L-lactide graft copolymers: effect of hydrophobic side chains on the physico-chemical properties and biodegradability. *Carbohydr. Polym.* **64**:254–266 (2006).
52. M. H. Boskabady and M. Saadatinejad. Airway responsiveness to beta-adrenergic agonist (Salbutamol) in asthma. *J. Asthma* **40**:917–925 (2003).
53. J. C. Leroux, E. Alleman, E. Doelker, and R. Gurny. New approach for the preparation of nanoparticles by an emulsification-diffusion method. *Eur. J. Pharm. Biopharm.* **41**:14–18 (1995).
54. D. Quintanar-Guerrero, H. Fessi, E. Allemann, and E. Doelker. Influence of stabilizing agents and preparative variables on the formation of poly(D,L-lactic acid) nanoparticles by an emulsification–diffusion technique. *Int. J. Pharm.* **143**:133–141 (1996).
55. S. Galindo-Rodriguez, E. Allemann, H. Fessi, and E. Doelker. Physicochemical parameters associated with nanoparticle formation in the salting-out, emulsification–diffusion, and nanoprecipitation methods. *Pharm. Res.* **21**:1428–1439 (2004).
56. S.-W. Choi, H.-Y. Kwon, W.-S. Kim, and J.-H. Kim. Thermodynamic parameters on poly(D,L-lactide-co-glycolide) particle size in emulsification–diffusion process. *Colloids Surf, A* **201**:283–289 (2002).
57. M. Trotta, D. Chirio, R. Cavalli, and E. Peira. Hydrophilic microspheres from water-in-oil emulsions by the water diffusion technique. *Pharm. Res.* **21**:1445–1449 (2004).
58. H.-Y. Kwon, J.-Y. Lee, S.-W. Choi, Y. Jang, and J.-H. Kim. Preparation of PLGA nanoparticles containing estrogen by emulsification-diffusion method. *Colloids Surf, A* **182**:123–130 (2001).
59. S. Galindo-Rodriguez, E. Allemann, E. Doelker, and H. Fessi. Versatility of three techniques for preparing ibuprofen-loaded methacrylic acid copolymer nanoparticles of controlled sizes. *J. Drug Delivery Sci. Tech.* **15**:347–354 (2005).
60. M. Liu, J. Dong, Y. Yang, X. Yang, and H. Xu. Characterization and release of triptolide-loaded poly(D,L-lactic acid) nanoparticles. *Euro. Polym. J.* **41**:375–382 (2005).
61. P. Begat, D. A. V. Morton, J. N. Staniforth, and R. Price. The cohesive-adhesive balances in dry powder inhaler formulations I: direct quantification by atomic force microscopy. *Pharm. Res.* **21**:1591–1597 (2004).
62. H. D. C. Smyth, V. P. Beck, D. Williams, and A. J. Hickey. The influence of formulation and spacer device on the in vitro performance of solution chlorofluorocarbon-free propellant-driven metered dose inhalers. *AAPS PharmSciTech.* **5**:1–7 (2004).
63. R. O. Williams III, A. M. Patel, M. K. Barron, and T. L. Rogers. Investigation of some commercially available spacer devices for the delivery of glucocorticoid steroids from a pMDI. *Drug Dev. Ind. Pharm.* **27**:401–412 (2001).
64. B. Forbes and C. Ernhardt. Human respiratory epithelial cell culture for drug delivery applications. *Eur. J. Pharm. Biopharm.* **60**:193–205 (2005).